Analytical Methods

ROYAL SOCIETY OF CHEMISTRY

PAPER

View Article Online
View Journal | View Issue

Cite this: *Anal. Methods*, 2021, **13**, 2005

A lanthanide-based ratiometric fluorescent biosensor for the enzyme-free detection of organophosphorus pesticides†

Tianlin Wang[ab] and Yaqing Liu *[ab]

Received 1st March 2021
Accepted 22nd March 2021

DOI: 10.1039/d1ay00345c

rsc.li/methods

Organophosphorus pesticides (OPs) residues have caused great concern as they cause great harm to public health. Herein, a ratiometric fluorescent sensing system was developed for the OPs detection with the merits of enzyme-free, simple operation, short-time and sensitivity. The change in the fluorescence signal in the sensing system was provided by guanine-rich DNA (G-DNA) and silver nanoparticles (AgNPs) with terbium ion (Tb^{3+}) and dured. Tb^{3+} coordinated with the G-DNA to form a DNA–Tb complex to emit green fluorescence, which can be significantly enhanced by AgNPs based on the mechanism of metal enhanced fluorescence. Dured embedded into the G-DNA emits red fluorescence as the built-in fluorescence signal. After adding OPs into the DNA–Tb–dured–AgNPs sensing system, the fluorescence of Tb^{3+} quenched, while the fluorescence of dured remained unchanged. The OPs detection is implemented enzyme-free or label-free and has the advantage of high sensitivity and reliability. The limit of detection reaches as low as 0.034 μg L^{-1}, and good recoveries are obtained for the OPs detection in tap water and apple. Moreover, the developed sensing system is simple in preparation and low cost, exhibiting an efficient platform to meet the requirement for *in situ* application in food safety and environmental monitoring.

1. Introduction

Organophosphorus pesticides (OPs) are widely used throughout the world and play an important role in improving the crop yield and reducing harvest losses due to their highly efficient insecticidal, bactericidal and herbicidal activities.[1–4] However, the wide use of OPs leads to their accumulation in soil, water, and agricultural products since OPs are difficult to be degraded. OPs even at low level cause great harm to human health and can result in numerous diseases such as Parkinson's disease, endocrine disruption, memory loss, proximal muscle weakness and anorexia.[5–8] According to the report of the World Health Organization, about one million OPs poisoning accidents occur annually.[9] Hence, the sensitive detection of OPs with high reliability is urgently required.

Diverse strategies have been developed to determine OPs, including enzyme-linked immunosorbent assay,[10] liquid chromatography-mass spectrometry,[11] gas chromatography-mass spectrometry,[12] and high-performance liquid chromatography.[13] These methods have advantages in terms of sensitivity and selectivity, while suffer from limitations such as requirement of expensive equipment, complicated and time-consuming procedures and the requirement of professionals. Thus, it is highly desirable to develop assays for convenient, low-cost, and rapid detection of OPs. In recent decades, considerable attention has been focused on constructing biosensors based on fluorescent,[14–16] colorimetric,[17–19] electrochemical,[20–22] and surface-enhanced Raman assays.[23,24] It is worth noting that most of the developed biosensors for OP detection are based on inhibiting the enzyme activity of acetylcholinesterase (AChE), which hinders their further application in *in situ* detection due to the high cost and critical requirement for reservation. Moreover, the developed assays usually rely on single signal channel that is readily interfered by the environment, excitation light source, instrument deviation and so on, which may result in false-positive or false-negative results.[25] Ratiometric sensing platform has self-calibration function and is considered as an effective solution for minimizing the interference and improving the analytical accuracy.[26,27]

Among the developed strategies, fluorescent assay is considered as a powerful way due to its advantages of sensitivity, non-invasive detection and possibility for remote operation.[28,29] Considering the high cost and complex operation of fluorophore labeling, it is necessary to construct enzyme-free and label-free biosensors. Lanthanide-doped nanomaterials

[a]*Beijing Advanced Innovation Center for Food Nutrition and Human Health, Beijing Technology and Business University, Beijing 100037, P. R. China*

[b]*State Key Laboratory of Food Nutrition and Safety, College of Food Engineering and Biotechnology, Tianjin University of Science and Technology, Tianjin 300457, P. R. China. E-mail: yaqingliu@tust.edu.cn*

† Electronic supplementary information (ESI) available. See DOI: 10.1039/d1ay00345c

are considered as excellent building blocks for biosensors due to their unique luminescence properties including narrow emission bandwidths, multiple emission bands, long luminescence lifetimes, and large Stokes/anti-Stokes.[30–32] Terbium(III) (Tb^{3+}), one of the lanthanide ions, exhibits fluorescence when coordinated with guanine-rich single-strand oligonucleotides (DNA–Tb) in that the energy is transferred from the DNA to Tb^{3+} once exposed under ultraviolet light.[33] Upon further coordination with silver nanoparticles (AgNPs), the fluorescence of the resultant DNA–Tb–AgNPs is significantly augmented based on the metal-enhanced fluorescence mechanism.[34,35] To construct a ratiometric fluorescent sensing system, dured with red fluorescence emission is used as an internal reference signal probe to integrate with DNA–Tb–AgNPs. In the presence of OPs, the lanthanide could be coordinated with the OPs, which results in the quenching of lanthanide fluorescence.[36–38] Moreover, the fluorescence of dured cannot be influenced. Thus, it is expected that the constructed sensing system could be realized for the ratiometric detection of OPs, which presents advantages of simple, fast, high sensitivity and low cost.

2. Materials and methods

2.1 Materials and instruments

The used DNA strands were synthesized by Sangon Biotech Co., Ltd (Shanghai, China) (Table S1 in ESI†). Terbium nitrate hexahydrate ($Tb(NO_3)_3 \cdot 6H_2O$, 99.99%), methyl parathion, omethoate, phosmet, dichlorvos, dursban and phorate were purchased from Aladdin Reagent Co. Ltd (Shanghai, China). Dured, PVP-K30 and glycerol were bought from Solabo Technology Co., Ltd (Beijing, China). Metal salts, ammonium hydroxide (30%), ascorbic acid and methanol were purchased from Kermel Reagent Co. Ltd (Tianjin, China). All the chemicals were of analytical grade. The water used was purified by Millipore Milli-Q (18 MΩ cm).

DNA concentrations were obtained according to the absorption values at 260 nm on a UV-2450 spectrophotometer (Shimadzu, Japan). The fluorescence spectra of Tb^{3+} and dured were recorded on an F-7000 fluorescence spectrometer (Hitachi, Japan). The morphology of AgNPs was characterized by a JEM-3010 transmission electron microscope (TEM) (Hitachi, Japan).

2.2 Preparation of AgNPs

The synthesis of AgNPs was based on a previous report with slight modification.[39] A glycerol–water mixture (40 vol% glycerol, 50 mL) was stirred in a 100 mL flask and heated up to 95 °C. Silver nitrate (9 mg) and sodium citrate (3%, 1.0 mL) were then added into the mixture, which was stirred for 1 h at 95 °C. After that, the colloid was stored at 4 °C. Water (138 mL), glycerol (23 mL) and PVP (0.58 g) were stirred in a 250 mL flask at room temperature. The colloid (14.4 mL) was added and then kept at room temperature for 20 s. Furthermore, a 0.29 mL diamine silver complex (20 mg silver nitrate in 1.0 mL water plus 220 mL ammonium hydroxide 30%) and ascorbic acid (9.2 mg) were added into the reaction system. After 1 h, the obtained AgNPs were stabilized with 6 g PVP and then washed with water for three times.

2.3 Preparation of the sensing system for OPs detection

The detection system was constructed by mixing Tb^{3+}, DNA, dured, and AgNPs in Tris–HCl buffer (pH = 7.5, 10 mM). The final concentrations of Tb^{3+}, DNA, dured, and AgNPs were 0.2 μM, 5.0 μM, 3.0 μM and 15 pM, respectively. For the detection of OPs, OPs with different concentrations were added into the system. Here, parathion methyl was used as a model sample. After incubating for 10 min, the fluorescence response of Tb^{3+} and dured were recorded on a fluorescence spectrometer. The fluorescence intensity ratio of Tb^{3+} at 545 nm (F_{Tb}) to dured (F_D) at 680 nm (F_{Tb}/F_D) was used as the readout signal.

2.4 Determination of OPs in real samples

OPs detection in a fruit sample followed the previous report with apple as the real sample.[40] The apples were chopped into pieces and then crushed into homogenates. The obtained homogenates were dissolved into 20 mL of buffer solution and stirred for 10 min. The apple juice was then filtered with a membrane to get rid of the insoluble matrixes. For the OPs detection in tap water, the tap water was centrifuged at 14 000 rpm for 10 min and then filtered with a nitrocellulose membrane (0.22 μm). OPs with different concentrations were then spiked into the samples. The fluorescence response was recorded after being incubated with the sensing system for 10 min.

3. Results and discussion

3.1 Fluorescence response of dured–DNA–Tb to OPs

With the fluorescence of DNA–Tb and dured–DNA as the detection signal and reference signal, respectively, a novel enzyme-free ratiometric sensor for the detection of OPs was developed, as shown in Fig. 1A. The detection strategy was validated by implementing the fluorescence experiments shown in Fig. 1B. No obvious fluorescence was monitored from the single-strand DNA (Fig. 1B(a)) and dured (Fig. 1B(b)). Dured embedded in the DNA forming dured–DNA complex emits red fluorescence with a characteristic peak at 680 nm (Fig. 1B(c)). The mixture of DNA and Tb^{3+} shows slight green fluorescence with two main characteristic peaks at 490 nm and 545 nm, respectively (Fig. 1B(d)). The integrated dured–DNA–Tb complex has the characteristic peaks originated from both dured and Tb^{3+} (Fig. 1B(e)). After introducing AgNPs, the fluorescence of Tb^{3+} in the resultant DNA–Tb–dured–AgNPs system is greatly enhanced due to the metal fluorescence enhancement effect of AgNPs, while the fluorescence of dured changes slightly (Fig. 1B(f)). When OPs were added into the DNA–Tb–dured–AgNPs sensing system, the coordination between OPs and Tb^{3+} prevents the energy transfer from DNA to Tb^{3+},[37,38] thus quenching the fluorescence of Tb^{3+}. However, the added OPs have slight influence on the fluorescence of dured (Fig. 1B(g)). With the fluorescence intensity ratio of Tb^{3+} at 545 nm (F_{Tb}) to dured (F_D) at 680 nm (F_{Tb}/F_D) as the readout signal, it was

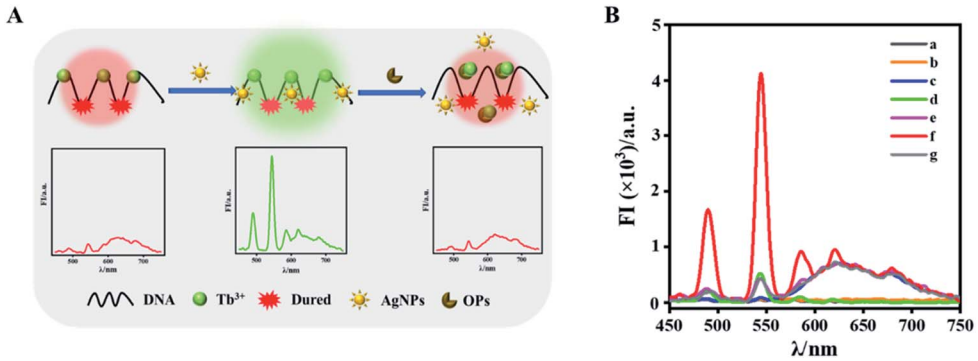

Fig. 1 (A) Schematic of the ratiometric fluorescence sensor of DNA–Tb–dured–AgNPs for organophosphorus pesticides (OPs) detection. (B) Fluorescence spectra of numerous systems: (a) DNA, (b) dured, (c) dured–DNA, (d) DNA–Tb, (e) DNA–Tb–dured, (f) DNA–Tb–dured–AgNPs, (g) DNA–Tb–dured–AgNPs + OPs.

further found that F_{Tb}/F_D decreases with the increase in concentration of OPs (see Fig. S1 in ESI†). The results validate the possibility of DNA–Tb–dured–AgNPs as a ratiometric fluorescent biosensor for the detection of OPs.

3.2 Optimization of experimental conditions

The sensitivity of the proposed biosensor is related to numerous factors, such as the DNA sequence, pH of the buffer solution, concentration of dured, the particle size and concentration of AgNPs, and incubation time of OPs. Thus, the optimal conditions were explored for the determination of OPs. According to the previous report, the amount and position of guanine in DNA effects the fluorescence enhancement of Tb^{3+}.[41] Here, nine single-strand DNAs with different sequences were used to sensitize the Tb^{3+} emitted fluorescence (F_{Tb}). After adding AgNPs, an enhanced fluorescence (F'_{Tb}) was monitored. A maximum ratio of F'_{Tb}/F_{Tb} at 545 nm was obtained from the DNA named as 20 GT (Fig. 2A). Moreover, the DNAs with

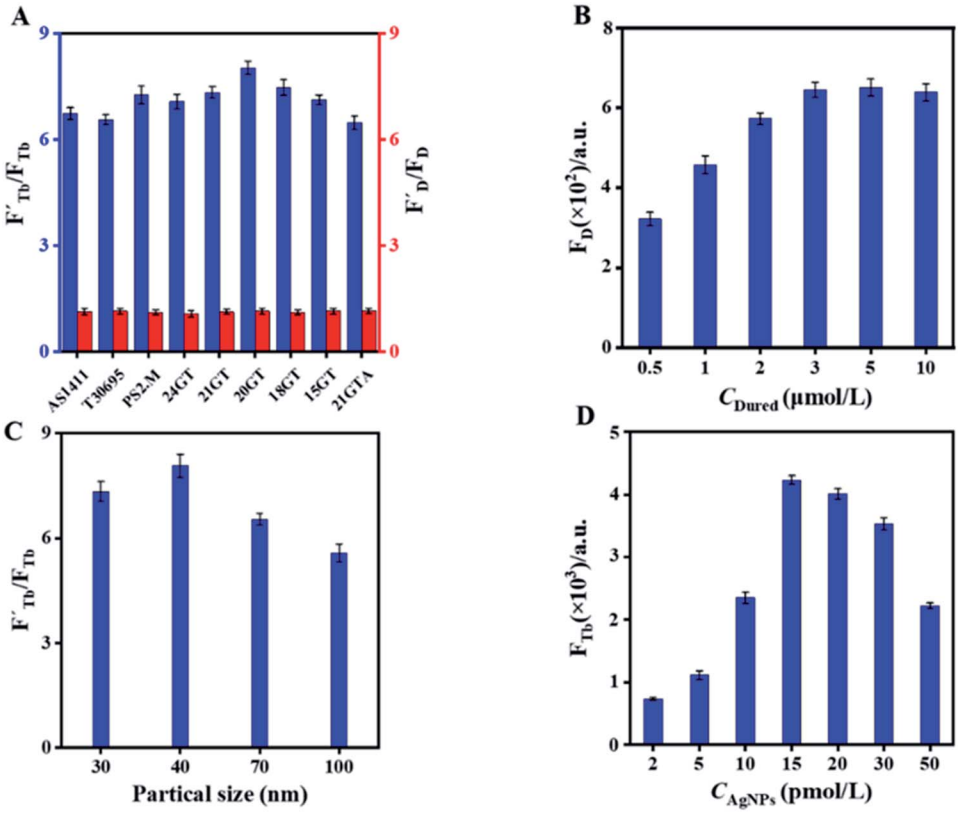

Fig. 2 (A) The effect of DNA with different base sequences on the fluorescence intensity of Tb^{3+} and dured. (B) The effect of the dured concentration on the fluorescence intensity of dured. (C) The effect of AgNPs with different particle sizes on the fluorescence of Tb^{3+}. (D) The effect of the concentration of AgNPs on the fluorescence intensity of Tb^{3+}.

different sequence have no obvious effects on the fluorescence response of dured. Thus, DNA with the 20 GT sequence was used for the construction of the sensing platform. In this case, the concentration of dured was further evaluated by monitoring the fluorescence intensity of dured at 680 nm, which increases and reaches a plateau once the concentration of dured is over 3 μM (Fig. 2B). Thus, the concentration of dured was fixed at 3 μM for the following experiments. In the developed sensing strategy, AgNPs plays critical function, which was used as the mediator to augment the fluorescence of Tb^{3+}. As illustrated in Fig. 2C, a maximum ratio of F'_{Tb}/F_{Tb} is obtained when the AgNP particle size is 40 nm (transmission electron micrograph of the AgNPs is shown in Fig. S2 in ESI†), where F'_{Tb} is the fluorescence intensity at 545 nm after adding AgNPs. Moreover, the F'_{Tb}/F_{Tb} increases with the increase in the concentration of the AgNPs from 2 pM to 15 pM (Fig. 2D). With further increase in concentration, however, the fluorescence intensity of Tb^{3+} decreases, which might be ascribed to the internal filtration effect of AgNPs.[42] Thus, the concentration of AgNPs was fixed at 15 pM for the following experiments.

According to the above results, the sensing system of DNA–Tb–dured–AgNPs was constructed. Subsequently, the influence of buffer pH of the OPs in the sensing system was further evaluated with F_{Tb}/F_D as the readout. As illustrated in Fig. 3A, the value of F_{Tb}/F_D increases with an increase in pH from 5.0 to 8.0 and then decreases when the pH is over 8.0. Thus, pH 8.0 was used in the following measurements. As illustrated in Fig. 3B, the addition of OPs results in the decrease of F_{Tb}/F_D, which quickly reaches minimum when the sensing system is exposed into the OPs environment for 10 min. Thus, 10 min was set as the optimal incubation time.

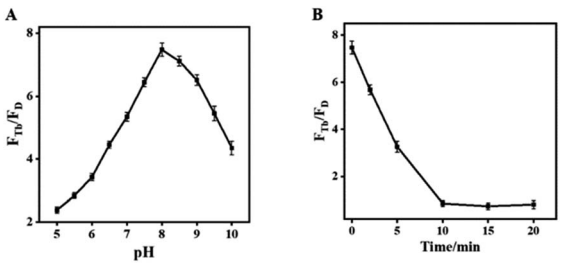

Fig. 3 (A) The effect of the buffer solution with different pH values on the fluorescence ratio of F_{Tb}/F_D. (B) The effect of different incubation times of OPs in the sensing system on F_{Tb}/F_D.

3.3 Sensitive detection of OPs

Before the detection of OPs, the stability of the detection system was evaluated with F_{Tb}/F_D as the readout. As shown in Fig. S3,† the value of F_{Tb}/F_D changed slightly even when the time was extended to 120 min in the environment, indicating excellent stability. Then, the detection sensitivity and linear detection range of the DNA–Tb–dured–AgNPs towards OPs were determined, under the optimal conditions. As illustrated in Fig. 4A, with the increase in the concentration of OPs, the fluorescence response of Tb^{3+} was decreased and the fluorescence response of dured was essentially unchanged. The fluorescence intensity ratio of Tb^{3+} at 545 nm (F_{Tb}) to dured (F_D) at 680 nm (F_{Tb}/F_D) was used as the readout signal. The F_{Tb}/F_D displays two linear relationships with the OPs concentration ranging from 0.03 μg L^{-1} to 5 μg L^{-1} and from 10 μg L^{-1} to 160 μg L^{-1} with good correlation coefficient of 0.992 and 0.995, respectively (Fig. 4B and C). The limit of detection (LOD) was found at 0.034 μg L^{-1} by calculating three times of the signal-to-noise ratio. Compared to the previous reports about the detection of OPs (Table S2 in ESI†), the enzyme-free and label-free sensing system presents advantages of simple operation, short-time and sensitive detection, showing a great potential application in actual detection. This strategy also can be applied for other OPs detection such as omethoate, phosmet, dichlorvos, dursban and phorate (Fig. S4 in ESI†).

3.4 The anti-interference capability of the sensing system

Anti-interference capability is a key factor in evaluating the performance of a sensor. To evaluate the specificity of the DNA–Tb–dured–AgNPs sensing system for the OPs detection, the influence of some potential interferences in food samples was

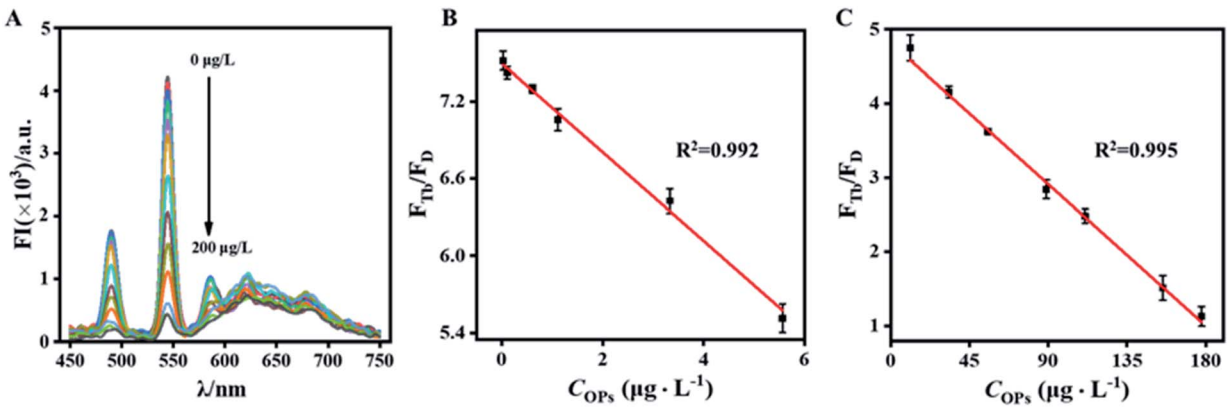

Fig. 4 (A) The fluorescence spectra of Tb^{3+} and dured as a function of OPs with different concentrations (0.01, 0.02, 0.03 0.1, 0.5, 1.0, 3.0, 5.0, 10, 20, 30, 40, 60, 80, 100, 120, 140, 160, 200 μg L^{-1}). The linear relationship between the F_{Tb}/F_D and OP concentrations within the range of 0.03–5.0 μg L^{-1} (B) and 10–160 μg L^{-1} (C).

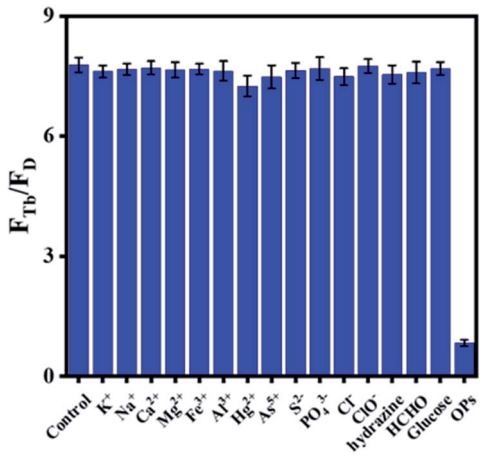

Fig. 5 Effects of other interfering substances on the fluorescence ratio (F_{Tb}/F_D) after being added into the DNA–Tb–dured–AgNPs sensing system (OPs: 100 μg L^{-1}. K^+, Na^+, Ca^{2+}, Mg^{2+}, Fe^{3+}, Cl^-, ClO^-, S^{2-}, PO_4^{3-}, glucose, hydrazine and HCHO: 3 μmol L^{-1}).

explored, including K^+, Na^+, Ca^{2+}, Mg^{2+}, Fe^{3+}, Al^{3+}, Hg^{2+}, As^{5+}, Cl^-, ClO^-, S^{2-}, PO_4^{3-}, glucose, hydrazine and formaldehyde (HCHO). As shown in Fig. 5, different from the effects of OPs, the potential interferences have negligible effects on the fluorescence response of the sensing system. The results validate that the developed biosensing system has excellent anti-interference capability.

3.5 Detection of OPs in real samples

Here, tape water and apple were used as real samples to evaluate the practical feasibility of the developed sensing system. No OPs was found in the pretreated samples. The standard addition method was then used to explore the practicability of the DNA–Tb–dured–AgNPs sensing system for the detection of OPs. As illustrated in Table 1, the spiked OPs in tap water can be measured with good recovery (from 97.0 to 102.0%) and acceptable relative standard deviation (RSD <3.1%). From Table 2, it can be seen that the spiked OPs in apple can be measured with good recovery (from 97.9 to 106.0%) and acceptable relative standard deviation (RSD <2.8%). The results validate that the developed sensing strategy has good performance for the detection of OPs in real samples.

Table 1 Determination of OPs in tap water

Sample	Spiked (μg L^{-1})	Detected (μg L^{-1})	Recovery (%)	RSD (%)
Tap water	0	0	—	—
	1.0	0.97 ± 0.03	97.0	3.1
	50	48.77 ± 0.53	97.5	1.1
	100	105.31 ± 1.41	102.0	1.3

Table 2 Determination of OPs in apple

Sample	Spiked (μg kg^{-1})	Detected (μg kg^{-1})	Recovery (%)	RSD (%)
Apple	0	0	—	—
	1.0	1.06 ± 0.03	106.0	2.8
	50	48.94 ± 0.59	97.9	1.2
	100	103.97 ± 1.94	103.9	1.9

4. Conclusion

A ratiometric fluorescence sensing system of DNA–Tb–dured–AgNPs for the sensitive detection of OPs has been successfully developed. The LOD reaches as low as 0.034 μg L^{-1}. The ratiometric sensing system has great advantages that make it great potential application. First, the sensing system is prepared by mixing the required chemical materials, and the preparation procedure is quite simple. Second, the sensing system is enzyme-free and label free, and the cost is quite low. Furthermore, the sensing system can resist the potential interference and has nice recovery for the detection of OPs in real samples. Last but not least, the developed sensing system may be explored as a general approach for the detection of OPs.

Conflicts of interest

There are no conflicts to declare.

Acknowledgements

This work is supported by the National Natural Science Foundation of China (No. 21775108 and 21575138).

Notes and references

1 G. Aragay, F. Pino and A. Merkoçi, *Chem. Rev.*, 2012, **112**, 5317–5338.
2 M. Eddleston and F. R. Chowdhury, *Br. J. Clin. Pharmacol.*, 2016, **81**, 462–470.
3 J. V. Kumar, R. Karthik, S. M. Chen, K. Natarajan, C. Karuppiah, C. C. Yang and V. Muthuraj, *ACS Appl. Mater. Interfaces*, 2018, **10**, 15652–15664.
4 E. A. Songa and J. O. Okonkwo, *Talanta*, 2016, **155**, 289–304.
5 M. Jokanović and M. Kosanović, *Environ. Toxicol. Pharmacol.*, 2010, **29**, 195–201.
6 A. A. Malekirad, M. Faghih, M. Mirabdollahi, M. Kiani, A. Fathi and M. Abdollahi, *Arh. Hig. Rada Toksikol.*, 2013, **64**, 1–8.
7 A. Cecchid, M. G. Rovedattia, G. Sabinoac and G. G. Magnarelliab, *Ecotoxicol. Environ. Saf.*, 2012, **80**, 280–287.
8 Y. Yi, G. Zhu, C. Liu, Y. Huang, Y. Zhang, H. Li, J. Zhao and S. Yao, *Anal. Chem.*, 2013, **85**, 11464–11470.
9 S. Syed, S. A. Gurcoo, A. K. Farooqui, W. Nisa, K. Sofi and T. M. Wani, *Saudi J. Anaesth.*, 2015, **9**, 49–54.
10 G. Qian, L. Wang, Y. Wu, Q. Zhang, Q. Sun, Y. Liu and F. Liu, *Food Chem.*, 2009, **117**, 364–370.
11 C. Yu, D. Hao, Q. Chu, T. Wang, S. Liu, T. Lan, F. Wang and C. Pan, *Food Chem.*, 2020, **21**, 126657.

12 A. Okamura, I. Saito, J. Ueyamad, Y. Ito, T. Nakajima and M. Kamijima, *Toxicol. Lett.*, 2012, **210**, 220–224.
13 D. Harshit, K. Charmy and P. Nrupesh, *Food Chem.*, 2017, **230**, 448–453.
14 T. Yao, A. Liu, Y. Liu, M. Wei, W. Wei and S. Liu, *Biosens. Bioelectron.*, 2019, **145**, 111705.
15 S. Huang, M. Guo, J. Tan, Y. Geng, J. Wu, Y. Tang, C. Su, C. C. Lin and Y. Liang, *ACS Appl. Mater. Interfaces*, 2018, **10**, 39056–39063.
16 Y. Cai, J. Fang, B. Wang, F. Zhang, G. Shao and Y. Liu, *Sens. Actuators, B*, 2019, **292**, 156–163.
17 T. Han and G. Wang, *J. Mater. Chem. B*, 2019, **7**, 2613–2618.
18 H. Ouyang, Q. Lu, W. Wang, Y. Song, X. Tu, C. Zhu, J. N. Smith, D. Du, Z. Fu and Y. Lin, *Anal. Chem.*, 2018, **90**, 5147–5152.
19 Y. Liu, B. Lv, A. Liu, G. Liang, L. Yin, Y. Pu, W. Wei, S. Gou and S. Liu, *Sens. Actuators, B*, 2018, **265**, 675–681.
20 W. Tang, J. Yang, F. Wang, J. Wang and Z. Li, *Anal. Chim. Acta*, 2019, **1060**, 97–102.
21 D. Song, X. Jiang, Y. Li, X. Lu, S. Luan, Y. Wang, Y. Li and F. Gao, *J. Hazard. Mater.*, 2019, **373**, 367–376.
22 F. Zhao, Y. Yao, X. Li, L. Lan, C. Jiang and J. Ping, *Anal. Chem.*, 2018, **90**, 11658–11664.
23 D. Huang, J. Zhao, M. Wang and S. Zhu, *Food Control*, 2020, **108**, 106835.
24 M. J. Tan, Z. Y. Hong, M. H. Chang, C. C. Liu, H. F. Cheng, X. J. Loh, C. H. Chen, C. D. Liao and K. V. Kong, *Biosens. Bioelectron.*, 2017, **96**, 167–172.
25 F. Wang, X. Hu, J. Hu, Q. Peng, B. Zheng and D. Xiao, *J. Mater. Chem. B*, 2018, **6**, 6008–6015.
26 J. Q. Chen, S. F. Xue, Z. H. Chen, S. Zhang, G. Shi and M. Zhang, *Biosens. Bioelectron.*, 2018, **100**, 526–532.
27 Y. Xia, L. Wang, J. Li, X. Chen, J. Lan, A. Yan, Y. Lei, S. Yang, H. Yang and J. Chen, *Anal. Chem.*, 2018, **90**, 8969–8976.
28 D. K. Dang, S. Chandrasekaran, Y. L. T. Ngo, J. S. Chung, E. J. Kim and S. H. Hur, *Sens. Actuators, B*, 2018, **255**, 3284–3291.
29 J. Chang, H. Li, T. Hou, W. Duan and F. Li, *Biosens. Bioelectron.*, 2018, **104**, 152–157.
30 X. Wang, H. Chang, J. Xie, B. Zhao, B. Liu, S. Xu, W. Pei, N. Ren, L. Huang and W. Huang, *Coord. Chem. Rev.*, 2014, **273**, 201–212.
31 J. Feng and H. Zhang, *Chem. Soc. Rev.*, 2013, **42**, 387.
32 K. Binnemans, *Chem. Rev.*, 2009, **109**, 4283–4374.
33 K. L. Fu and C. Turro, *J. Am. Chem. Soc.*, 1999, **121**, 1–7.
34 C. Vietz, I. Kaminska, M. S. Paz, P. Tinnefeld and G. P. Acuna, *ACS Nano*, 2017, **11**, 4969–4975.
35 P. Liu, Y. Zhou, M. Guo, S. Yang, O. Félix, D. Martel, Y. Qiu, Y. Ma and G. Decher, *Nanoscale*, 2018, **10**, 848–855.
36 J. Feng and H. Zhang, *Chem. Soc. Rev.*, 2013, **42**, 387.
37 H. Zhang, X. Hua, X. Tuo, C. Chen and X. Wang, *J. Rare Earths*, 2012, **30**, 1203–1207.
38 H. X. Zhang, R. B. Wei, C. Z. Chen, X. L. Tuo and X. G. Wang, *Chin. Chem. Lett.*, 2015, **26**, 39–42.
39 D. Steinigeweg and S. Schlücker, *Chem. Commun.*, 2012, **48**, 8682–8684.
40 X. Meng, J. Wei, X. Ren, J. Ren and F. Tang, *Biosens. Bioelectron.*, 2013, **47**, 402–407.
41 M. Zhang, H. N. Le, X. Q. Jiang, B. C. Yin and B. C. Ye, *Anal. Chem.*, 2013, **85**, 11665–11674.
42 J. Zhang, R. Zhou, D. Tang, X. Hou and P. Wu, *TrAC, Trends Anal. Chem.*, 2019, **110**, 183–190.

